BUNSEN-MAGAZIN · 28. JAHRGANG · 5/2026

Björn Corzilius

Dynamic nuclear polarization: Metal-ion polarizing agents and site-specific enhancement

Dynamic nuclear polarization (DNP) has been first proposed by Albert Overhauser in 1953: By irradiation of the conduction electron spin resonance in lithium metal the ^{7}Li nuclear spins should become hyperpolarized [1]. After some controversy involving several Nobel laureates in how far his hypothesis is in conflict with the second law of thermodynamics [2], Charles Slichter together with his PhD student Thomas Carver performed the experiment and recorded the first DNP-enhanced NMR spectrum of ^{7}Li in the same year [3]. This discovery of what we now call the Overhauser effect (OE) has ignited an exciting field of interdisciplinary research, encompassing high-frequency electrical engineering, radical chemistry, and magnetic resonance methods development. While still advancing at a fast rate, DNP-enhanced NMR has matured into an established method with fully commercially available instrumentation, enabling applications of NMR in both liquid and solid state to problems in biochemistry and materials science which would otherwise suffer from the low thermal nuclear spin polarization and would thus be impossible due to excessive experimental duration [4-6].

DNP mechanisms

In thermal equilibrium, the nuclear polarization of a spin-1/2 particle is given by the Boltzmann distribution:

$$P = \frac{N_\alpha - N_\beta}{N_\alpha + N_\beta} = \tanh\left(\frac{\gamma\hbar B_0}{2k_\mathrm{B}T}\right) \qquad (1)$$

In the high-temperature limit, where the thermal energy is significantly larger than the Zeeman energy (i.e., $\gamma\hbar B_0 \ggg k_\mathrm{B}T$), this polarization scales linearly with the gyromagnetic ratio, and thus, the spin of unpaired (nearly) free electrons is, for example, 658 times larger than that of ^{1}H nuclei. In theory, the NMR signal enhancement factor, ε, is limited by this ratio; in practice, two orders of magnitude may still be obtained due to relaxation losses and inefficiencies of the transfer process, resulting in acquisition time savings of up to four orders of magnitude. As the transfer of polarization from electrons to nuclei is neither energy conserving nor spontaneous, additional manipulation of the hyperfine-coupled electron-nuclear spin pair is required. Such manipulations must satisfy the following conditions: (1) the whole process must be net energy neutral and (2) an entropic driving force must be present in order to drive the transfer.

In the above-introduced OE, energy exchange with the lattice is enabled through fluctuations in the hyperfine interaction (HFI) caused by either molecular motion in solution [7] or transient interaction with conduction electrons in metals [1]. In non-conducting solids, such HFI fluctuations are frozen out and the OE is thus usually ineffective; however, it may still be enabled by local molecular dynamics such as the three-fold symmetric reorientation of methyl groups [8] or by vibronic coupling in mixed-valence radicals [9]. In all cases, these HFI fluctuations drive electron-nuclear cross-relaxation transitions which may lead to the accumulation of nuclear hyperpolarization during saturation of the electron paramagnetic resonance (EPR) transition by microwave irradiation (Fig. 1).

In the solid effect (SE) [10], direct excitation of the nominally forbidden electron-nuclear double quantum (DQ) or zero quantum (ZQ) transitions drives the polarization transfer (Fig. 1). This requires off-resonance excitation of the EPR spectrum at either the sum or the difference of the electron and nuclear Larmor frequencies ($\omega_{\mu w} = \omega_{0S} \pm \omega_{0I}$). Furthermore, the SE is dependent on non-averaged dipolar HFI which is only present in solids, but may also occur in viscous solutions [11].

A third mechanism, cross effect (CE) [10], is utilizing the coupling to a second electron spin matching in frequency thus that their Larmor frequency difference equals the nuclear Larmor frequency ($|\omega_{0S,1} - \omega_{0S,2}| = \omega_{0I}$). This enables energy conserving three-spin flips which then drive the nuclear hyperpolarization under selective EPR saturation of one of the electron spins. CE typically requires tailored biradical polarizing agents, but is highly efficient in the solid state under MAS because the three involved events – the microwave saturation event, the CE electron–electron–nuclear three-spin flip event, and the electron–electron flip-flop event – may be temporally decoupled and will occur consecutively for most spin packets during the MAS rotor period [12, 13]. This makes CE technically independent of microwave irradiation: while the SE fundamentally requires microwaves for driving the electron–nuclear transitions, the CE three-spin flips also occur in their absence and strongly link the nuclear polarization to the polarization difference between the two coupled

Prof. Dr.-Ing. Björn Corzilius
Institute of Chemistry
University of Rostock
Albert-Einstein-Str. 27, D-18059 Rostock
bjoern.corzilius@uni-rostock.de

DOI-Nr.: 10.26125/s5qf-rg13

Zurück zum Inhaltsverzeichnis

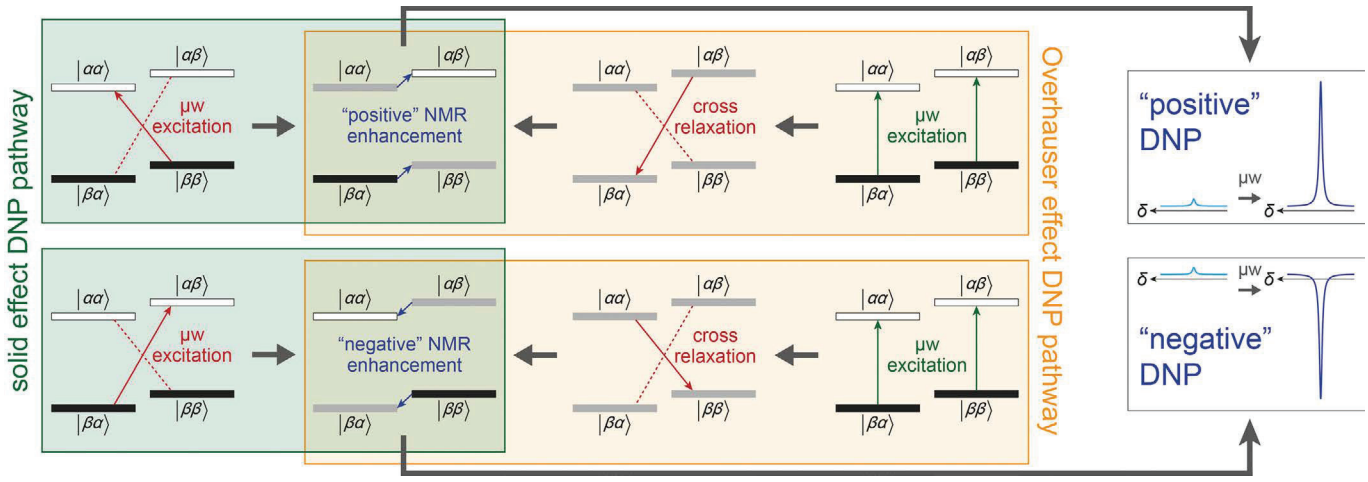

Fig. 1: Schematic representation of the DNP principle on a four-level system of a $S = 1/2$, $I = 1/2$ electron–nuclear two-spin system. Possible transitions are depicted by colored arrows: EPR (single quantum, SQ), green; NMR (SQ), blue; electron–nuclear DQ or ZQ, red. State populations (boxes) are coded by filling (black: strongly populated; white: weakly populated). Solid effect (coherent) and Overhauser effect (incoherent) DNP pathways demonstrate general principles for creating positive or negative DNP each; pathways starts at the far left or right from a system in thermal equilibrium. Gray states are medium populated as a result of saturation in a preceding step. Reprinted with permission from Biedenbänder et al. [6]. Copyright 2022 American Chemical Society.

electron spins. Thus, any manipulation of the electron–electron polarization difference results in changes to the nuclear polarization: selective saturation causes nuclear hyperpolarization, while convergence of the electron polarization may cause nuclear depolarization below the thermal equilibrium value [14, 15]. In practice, microwave irradiation is still the method of choice for achieving the polarization imbalance. Another mechanism, thermal mixing (TM), manifests under rather extreme conditions (very low temperatures and large radical concentrations) and is based on the same fundamental three-spin flips as is CE [10].

In solution, polarization is transferred from a polarizing agent carrying the unpaired electron(s) to a molecular analyte via transient interactions during translational and rotational diffusion and therefore, molecular diffusion is responsible for transporting the hyperpolarization through space. In solids, once the electron spin polarization has been transferred to a directly HFI-coupled nuclear spin, it may further evolve by homonuclear spin diffusion or heteronuclear cross relaxation. The former is typically used if polarization shall uniformly spread over the whole sample before being transferred by cross polarization to the nuclear species to be detected. This is called indirect DNP (see Figure 2) and allows sensitivity-enhanced NMR of analytes which are rather far removed from the polarizing agent, with minimal impact on linewidth and transversal relaxation from paramagnetic relaxation enhancement (PRE). This process is highly efficient for a dense network of ^{1}H due to its large gyromagnetic ratio and high abundance, and may become prohibitively slow for a sparse network of low-γ nuclei such as ^{13}C or ^{15}N in natural isotope abundance. This spreading of hyperpolarization by spin-diffusion is also the basis of surface-enhanced NMR spectroscopy by DNP (DNP-SENS) [16] and DNP of microcrystalline solids [17] (see "Exogenous DNP" in Figure 2). If a spatial relationship between polarizing agent and the region of interest (e.g., by paramagnetic labeling) is to be utilized for site-specific DNP [18], care has to be taken that hyperpolarization is not leaking uncontrollably into the bulk of the sample matrix, for example by perdeuteration of the solvent or by utilizing direct DNP of sparse low-γ nuclei [19] (Figure 2).

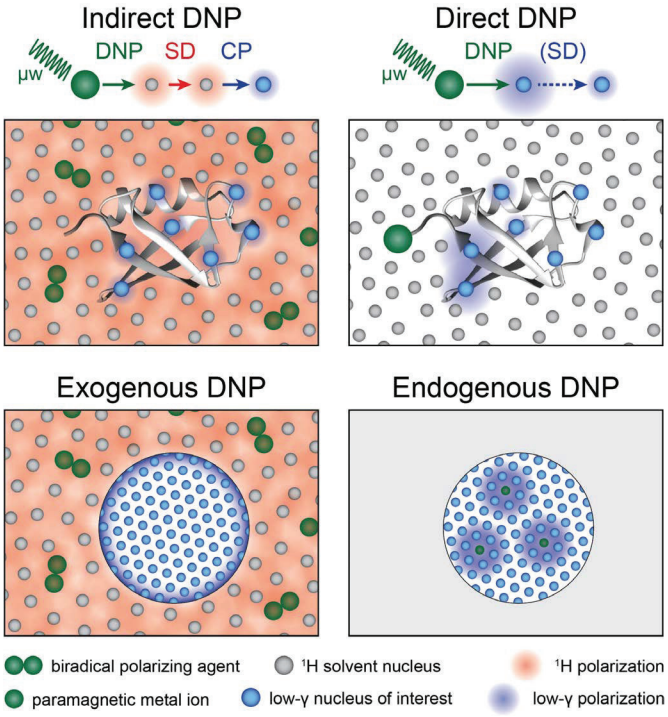

Fig. 2: Illustration of the general principles of indirect and direct DNP as well as exogenous and endogenous DNP. In indirect DNP, nuclear polarization emerging from biradicals is spread typically through the ^{1}H network by spin diffusion (SD) and then transferred to the nuclear species of interest by cross polarization (CP). In direct DNP (on the example of a biomolecule labeled with a metal-ion polarizing agent), the low-γ nuclei are directly hyperpolarized and SD is inefficient. In exogenous DNP, the analyte material is indirectly hyperpolarized through CP from the solvent containing a biradical polarizing agent, while in endogenous DNP the material is hyperpolarized by direct DNP from metal-ion polarizing agent doped into its lattice.

Polarizing agents: (bi)radicals or metal ions

As explained above, DNP requires a source of electron spin polarization. In most cases, persistent radicals are highly efficient and versatile polarizing agents. Carbon-centered radicals such as trityl (triarylmethyl, TAM) derivatives or α,γ-bisdiphe-

nylen-β-phenylallyl (BDPA, Koelsch radical) perform well for SE DNP of ^{1}H, as their EPR linewidths are sufficiently narrow even at high magnetic fields; this avoids overlap of the electron–nuclear ZQ and DQ transitions, ensuring efficient, selective excitation without cancellation which would otherwise occur in the differential solid effect [10]. Besides simple nitroxides such as TEMPO, they also perform well for OE DNP in solution, as their EPR line can be easily saturated [20]. For CE, bis-nitroxides or mixed biradicals consisting of a nitroxide and a trityl or BDPA moiety feature superior performance [21]. Nitroxides have been a cornerstone for the development of CE polarizing agents since their EPR spectrum is dominated by *g* anisotropy at high magnetic field, spanning ~100 MHz/T; this ensures that at any magnetic field the CE matching condition can be fulfilled.

Paramagnetic metal ions have been introduced as polarizing agents already in the early days of DNP, but have been rediscovered for applications in solids at high magnetic fields in the early 2010's [22]. Theoretical considerations predict that some metal ions may also be effective for OE DNP in solutions, however, reaching a significant saturation of the electron spin is prohibitive with the current state of the art microwave technology [23]. In solids, one problem often confronted with is the rather large breadth of their EPR spectra due to significant *g* anisotropy and/or zero-field splitting (ZFS). Commercial DNP spectrometers operate with a fixed microwave frequency and are limited in magnetic field sweep range, restricting the space of polarizing agents to those with an EPR resonance close to that of a free electron (i.e., $g \approx 2.01...1.99$). For example, Cu^{2+} with $S = 1/2$ features a relative *g* anisotropy on the order of 20% (i.e., $g_{\parallel} \approx 2.4$, $g_{\perp} \approx 2.0$), resulting in an EPR spectral breadth of ~50 GHz at a field of 9.4 T, while the ZFS of Fe^{3+} ($S = 5/2$) can assume several tens up to even hundreds of GHz. Thus, significant spectral excitation of the DNP-driving spin transitions is practically impossible. To date, only select paramagnetic metal ions have successfully been utilized as polarizing agents, including Gd^{3+} ($S = 7/2$) and high-spin Mn^{2+} ($S = 5/2$), which both feature half-filled electronic subshells (i.e., f^7 and d^5, respectively), and thus spin-only atomic states (i.e., $^{8}S_{7/2}$ and $^{6}S_{5/2}$, respectively) with maximum spin multiplicity following Hund's rule. Even though they feature a significant ZFS of several hundreds of MHz up to several GHz, their central EPR transition (i.e., $m_S = -1/2 \leftrightarrow +1/2$) is only affected in second order. This preserves effective central transition (CT) linewidths similar to those of narrow-line radicals such as trityl or BDPA. Tailored design for a highly symmetric ligand sphere can even result in extremely small ZFS of ~400 MHz, with up to 350-fold enhancement of ^{15}N signals by direct SE DNP [24]. The correlation between DNP efficiency and CT broadening by second-order ZFS together with HFI splitting due to the metal nucleus has recently been generalized by comparing isoelectronic Gd^{3+} and Eu^{2+} [25]. To date, most high-field applications of metal-ion polarizing agents have been performed with such S-type high-spin systems because doublet systems become incompatible with commercial DNP systems at high field due to their disadvantageous scaling of *g* anisotropy broadening. A noteworthy exemption is V^{4+} which has a nearly isotropic EPR resonance with $g \approx 1.98$ – although a custom-built DNP spectrometer was required to reach the SE matching condition [26].

Applications with metal-ion polarizing agents and site-specific DNP

Metal-ions offer exciting prospects as endogenous polarizing agents. The first demonstration of endogenous DNP in a biomolecule was performed with the protein flavodoxin where the flavin mononucleotide (FMN) co-factor was used in its reduced semiquinone form [27]. As such endogenous radical sites are both rare and difficult to generate or stabilize, this method is limited to very few amenable cases. In contrast, metal-ion co-factors are much more common to exist either in a natural paramagnetic state, or a diamagnetic ion may be substituted by a paramagnetic analog with often minimal impact on structure and function. Such a model case is the hammerhead ribozyme, a catalytically active RNA enzyme playing a crucial role in viral replication through cleavage of a substrate RNA strand upon infection of the host cell. As both Mg^{2+} or Mn^{2+} may act as catalytic co-factor for the cleavage reaction, Mn^{2+} can be used as an endogenous polarizing agent for direct ^{13}C SE, resulting in an 8-fold increase in NMR signal intensity; furthermore, it could be shown that this hyperpolarization can be maintained within the Mn^{2+}-carrying biomolecule with minimal leakage to other molecules [28]. In a follow-up study, qualitative evidence of distance-dependence between Mn^{2+} and the ^{13}C-labeled nucleotides could be obtained by comparison of different isotope-labeling patterns [29].

The initial DNP transfer process from the electron spin of the polarizing agent to a nuclear spin receiver in its direct vicinity relies on the dipolar hyperfine interaction and thus – following Fermi's Golden Rule – should impose a r^{-6} scaling on the transfer rate, where *r* is the electron–nuclear distance. Against simple intuition (i.e., faster transfer should lead to higher accumulated polarization), this does not directly relate to higher enhancement factors with decreasing electron–nuclear distance as PRE in fact follows the same inverse power law. Indeed, it has been shown that the enhancement factor is distance independent as long as PRE is the dominant nuclear relaxation mechanism [30, 31]. Nevertheless, the DNP rate constant itself, that is the rate with which enhanced polarization is accumulated, reports directly on the electron–nuclear distance as we have been able to demonstrate on different Gd-labeled ubiquitin mutants: By a combination of direct ^{15}N metal-ion DNP in a frozen solution, PRE experiments in solution at ambient temperature, as well as computational modeling, it was possible to statistically analyze the build-up rate for different amino acid residues and correlate them with their spatial distribution around the Gd-DOTA-maleimide polarizing agent tag (Fig. 3) [31]. Further experiments on lipid-embedded distance rulers with varying Gd^{3+}–^{15}N distances are currently underway, enabling new methods for measuring interatomic distances in the 12 to ~30 Å range.

Paramagnetic metal ions can also be ideal polarizing agents for crystalline solids as they may be sub-stoichiometrically doped into a diamagnetic lattice or may even be occurring naturally in materials of interest. This concept has been first demonstrated at high magnetic field on a co-crystalline lattice of $[Co(en)_3Cl_3]_2{\cdot}NaCl{\cdot}6H_2O$ (en = ethylenediamine) doped with Cr^{3+} (d^3, $S = 3/2$), allowing for direct SE DNP of ^{13}C and ^{59}Co

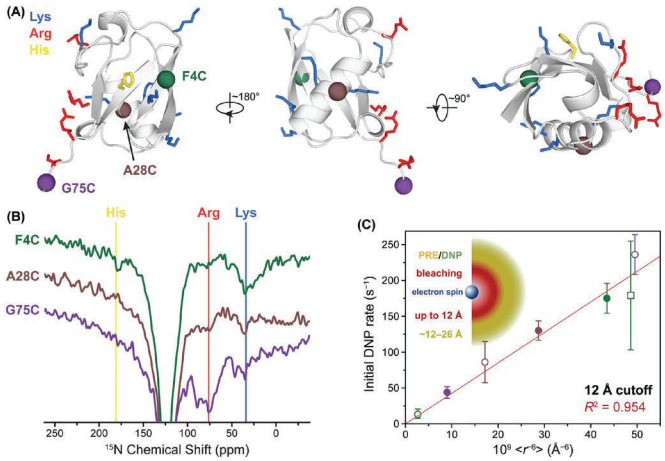

Fig. 3: Site-specific direct DNP in Gd^{3+}-labeled ubiquitin. (A) Graphical depiction of labeling positions as well as the positions of the amino acid side chains with resolved ^{15}N signals. (B) Direct ^{15}N DNP-enhanced spectra of all three Gd-labeled mutants. (C) Plot of the experimentally measured initial DNP rate versus the effective (inverse) Gd^{3+}–^{15}N distance calculated from distributed spin pairs within computational structure models as is described in the original publication [31]. Spin pairs with a distance below the cutoff of 12 Å are excluded; these pairs are expected to be situated within the bleaching volume of Gd^{3+}, while ^{15}N in a distance range between 12-26 Å are contributing to the detected signal.

(I = 7/2) [32]. This concept has been extended by the group of Michal Leskes at the Weizmann Institute of Science [33], and has been successfully applied for the study of battery materials, metal-organic frameworks, ceramics, and semiconductor nanocrystals [34]. A combination of exo- and endogenous DNP (see Figure 2) is particularly powerful for elucidating the morphology of the solid electrolyte interface (SEI): while endogenous DNP using metal-ion polarizing agent dopants highlights the NMR signature of the inorganic shell close to the bulk anode material, exogenous DNP using a biradical-containing wetting medium is able to selectively hyperpolarize the organic shell in direct contact with the electrolyte [35], as is demonstrated in Fig. 4.

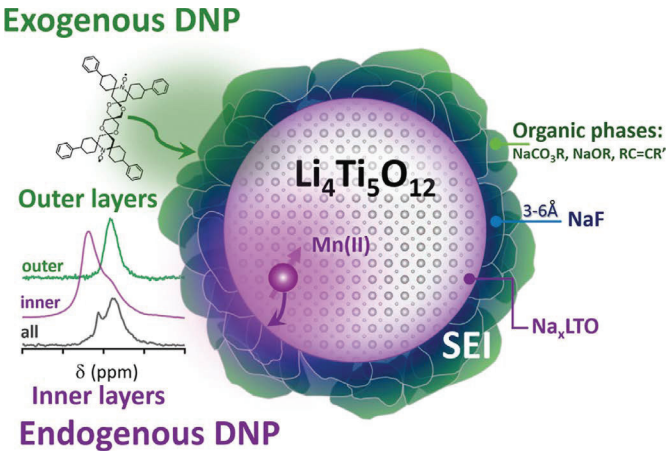

Fig. 4: Structural model of native SEI formed in LTO during cycling based on data acquired with different polarization sources and correlation experiments. The outer SEI, detected by exogenous DNP, is predominantly organic compounds (green) whereas the inner SEI, detected with endogenous DNP, is more inorganic (dark blue). NaF is the main inorganic species estimated to form a thin layer at the inner SEI. Na_xLTO formed due to Li–Na exchange at the outer layers of the particles is shown in dark purple. Figure and caption reproduced from Steinberg et al. [35], licensed under CC-BY 4.0.

Conclusion and outlook

DNP has become a standard method in advanced NMR studies, particularly for sensitivity enhancement in solids. For solution NMR, OE DNP is currently experiencing a breakthrough since the first commercially available solution-DNP probe has become available for applications at 9.4 T (400 MHz ^1H frequency) [36]. Interdisciplinary developments are still occurring rapidly, covering advances in polarizing agents, instrumentation and methods. On the one hand, metal-ion DNP has shown significant potential for endogenous as well as site-specific DNP, due to the ability of paramagnetic ions to integrate into the lattice of materials or into the binding site of a biomolecule with, in many cases, minimal interference with structure and/or function. Additionally, they are interesting polarizing agents for pulsed DNP due to the higher transition moments found in these high-spin systems. On the other hand, they are susceptible to small variations in ligand-field symmetry causing significant line broadening and are subject to relatively fast electron spin relaxation dynamics which require tailored design of chelates and impedes their application for OE DNP in solution. In any way, many developments will occur in the future regarding metal-ion and site-specific DNP, given that several of the most creative DNP laboratories worldwide are currently involved in active research into these directions.

References

[1] A. W. Overhauser, *Phys. Rev.* 1953, **92**, 411.

[2] C. P. Slichter, *Phys. Chem. Chem. Phys.* 2010, **12**, 5741.

[3] T. R. Carver and C. P. Slichter, *Phys. Rev.* 1953, **92**, 212.

[4] A. S. Lilly Thankamony, J. J. Wittmann, M. Kaushik, B. Corzilius, *Prog. Nucl. Magn. Reson. Spectrosc.* 2017, **102-103**, 120.

[5] A. G. M. Rankin, J. Trebosc, F. Pourpoint, J.-P. Amoureux, O. Lafon, *Solid State Nucl. Magn. Reson.* 2019, **101**, 116.

[6] T. Biedenbänder, V. Aladin, S. Saeidpour, B. Corzilius, *Chem. Rev.* 2022, **122**, 9738.

[7] K. H. Hausser and D. Stehlik, *Adv. Magn. Reson.* 1968, **3**, 79.

[8] F. A. Perras, D. F. Flesariu, S. A. Southern, C. Nicolaides, J. D. Bazak, N. M. Washton, T. Trypiniotis, C. P. Constantinides, P. A. Koutentis, *J. Phys. Chem. Lett.* 2022, **13**, 4000.

[9] S. Pylaeva, P. Marx, G. Singh, T. D. Kühne, M. Roemelt, H. Elgabarty, *J. Phys. Chem. A* 2021, **125**, 867.

[10] W. T. Wenckebach, *J. Magn. Reson.* 2019, **299**, 124.

[11] A. A. Kuzhelev, V. Denysenkov, I. M. Ahmad, O. Y. Rogozhnikova, D. V. Trukhin, E. G. Bagryanskaya, V. M. Tormyshev, S. T. Sigurdsson, T. F. Prisner, *J. Am. Chem. Soc.* 2023, **145**, 10268.

[12] F. Mentink-Vigier, Ü. Akbey, Y. Hovav, S. Vega, H. Oschkinat, A. Feintuch, *J. Magn. Reson.* 2012, **224**, 13.

[13] K. R. Thurber and R. Tycko, *J. Chem. Phys.* 2012, **137**, 084508.

[14] F. Mentink-Vigier, S. Paul, D. Lee, A. Feintuch, S. Hediger, S. Vega, G. De Paepe, *Phys. Chem. Chem. Phys.* 2015, **17**, 21824.

[15] K. R. Thurber and R. Tycko, *J. Chem. Phys.* 2014, **140**, 184201.

[16] A. Lesage, M. Lelli, D. Gajan, M. A. Caporini, V. Vitzthum, P. Miéville, J. Alauzun, A. Roussey, C. Thieuleux, A. Mehdi, G. Bodenhausen, C. Copéret, L. Emsley, *J. Am. Chem. Soc.* 2010, **132**, 15459.

[17] A. J. Rossini, A. Zagdoun, F. Hegner, M. Schwarzwälder, D. Gajan, C. Copéret, A. Lesage, L. Emsley, *J. Am. Chem. Soc.* 2012, **134**, 16899.

[18] R. Rogawski and A. E. McDermott, *Arch. Biochem. Biophys.* 2017, **628**, 102.

[19] V. Aladin and B. Corzilius, *eMagRes* 2020, **9**, 239.

[20] E. Ravera, C. Luchinat, G. Parigi, *J. Magn. Reson.* 2016, **264**, 78.

[21] R. Wei, G. Casano, Y. Zhang, I. M. Gierbolini-Colón, Y. Rao, S. S. Gunaga, F. J. Scott, J. Zhou, S. Chatterjee, S. Kumari, H. Karoui, M. Huang, S. T. Sigurdsson, G. De Paëpe, Y. Liu, F. Mentink-Vigier, A. Venkatesh, O. Ouari, L. Emsley, *Angew. Chem. Int. Ed.* 2025, **64**, e202505944.

[22] B. Corzilius, A. A. Smith, A. B. Barnes, C. Luchinat, I. Bertini, R. G. Griffin, *J. Am. Chem. Soc.* 2011, **133**, 5648.

[23] C. Luchinat, G. Parigi, E. Ravera, *J. Biomol. NMR* 2014, **58**, 239.

[24] G. Stevanato, D. J. Kubicki, G. Menzildjian, A.-S. Chauvin, K. Keller, M. Yulikov, G. Jeschke, M. Mazzanti, L. Emsley, *J. Am. Chem. Soc.* 2019, **141**, 8746.

[25] F. Taube, M. Reinhard, M. Bennati, B. Corzilius, *Analysis & Sensing* 2026, **6**, e70078.

[26] S. K. Jain, C.-J. Yu, C. B. Wilson, T. Tabassum, D. E. Freedman, S. Han, *Chem* 2021, **7**, 421.

[27] T. Maly, D. Cui, R. G. Griffin, A.-F. Miller, *J. Phys. Chem. B* 2012, **116**, 7055.

[28] P. Wenk, M. Kaushik, D. Richter, M. Vogel, B. Suess, B. Corzilius, *J. Biomol. NMR* 2015, **63**, 97.

[29] D. Daube, M. Vogel, B. Suess, B. Corzilius, *Solid State Nucl. Magn. Reson.* 2019, **101**, 21.

[30] D. Jardón-Álvarez, G. Reuveni, A. Harchol, M. Leskes, *J. Phys. Chem. Lett.* 2020, **11**, 5439.

[31] J. Heiliger, T. Matzel, E. C. Çetiner, H. Schwalbe, G. Kuenze, B. Corzilius, *Phys. Chem. Chem. Phys.* 2020, **22**, 25455.

[32] B. Corzilius, V. K. Michaelis, S. A. Penzel, E. Ravera, A. A. Smith, C. Luchinat, R. G. Griffin, *J. Am. Chem. Soc.* 2014, **136**, 11716.

[33] I. B. Moroz, Y. Feldman, R. Carmieli, X. Liu, M. Leskes, *Chem. Sci.* 2024, **15**, 336.

[34] D. Jardón-Álvarez and M. Leskes, *Prog. Nucl. Magn. Reson. Spectrosc.* 2023, **138-139**, 70.

[35] Y. Steinberg, E. Sebti, I. B. Moroz, A. Zohar, D. Jardón-Álvarez, T. Bendikov, A. Maity, R. Carmieli, R. J. Clément, M. Leskes, *J. Am. Chem. Soc.* 2024, **146**, 24476.

[36] M. Levien, L. Yang, A. van der Ham, M. Reinhard, M. John, A. Purea, J. Ganz, T. Marquardsen, I. Tkach, T. Orlando, M. Bennati, *Nat. Commun.* 2024, **15**, 5904.

Prof. Dr.-Ing. Björn Corzilius

Björn Corzilius studied chemistry at the TU Darmstadt. In the group of Klaus-Peter Dinse he investigated the electronic properties of carbon nanotubes by EPR and non-resonant microwave absorption; for that he earned his Ph.D. with distinction (summa cum laude) in 2008. Afterwards, he joined Robert G. Griffin at the Francis Bitter Magnet Laboratory at MIT for postdoctoral research on dynamic nuclear polarization. Supported by a DFG Emmy Noether Fellowship, he established his own research group at the Goethe University Frankfurt in 2013. In 2016, he was awarded with the Felix-Bloch-Lecture by the Magnetic Resonance Division (FGMR) of the GDCh, and in 2019 he was appointed Professor (W2) for physical chemistry with a focus on solid-state NMR spectroscopy at the University of Rostock.